

## Distinct metabolic phenotype renders $\beta$ -catenin mutant hepatocellular carcinoma susceptible to treatment-induced ischemia

Kelley Weinfurter<sup>1</sup>, Jennifer A. Crainic<sup>2</sup>, David Tischfield<sup>3</sup>, Daniel Ackerman<sup>3</sup>, Martin Kurian<sup>4</sup>, Abashai Woodard<sup>3</sup>, Wuyan Li<sup>3</sup>, Isabela Gatmaytan<sup>3</sup>, David Ostrowski<sup>4</sup>, Michael C. Soulen<sup>3</sup>, Mandeep Dagli<sup>3</sup>, Susan Shamimi-Noori<sup>3</sup>, Jeffrey Mondschein<sup>3</sup>, Deepak Sudheendra<sup>3</sup>, S. William Stavropoulos<sup>3</sup>, Shilpa Reddy<sup>3,5</sup>, Tamim Khaddash<sup>6</sup>, Emma E. Furth<sup>7</sup>, Evan S. Siegelman<sup>3</sup>, Stephen J. Hunt<sup>3</sup>, Gregory J. Nadolski<sup>3</sup>, David Kaplan<sup>1,5</sup>, Terence P.F. Gade<sup>3,5,8</sup>

<sup>1</sup>Division of Gastroenterology and Hepatology, University of Pennsylvania, Philadelphia, PA

<sup>2</sup>Human Biology Division, Fred Hutchinson Cancer Center, Seattle, WA

<sup>3</sup>Department of Radiology, University of Pennsylvania, Philadelphia, PA

<sup>4</sup>Perelman School of Medicine, University of Pennsylvania, Philadelphia, PA

<sup>5</sup>Corporal Michael J Crescenz VA Medical Center, Philadelphia, PA

<sup>6</sup>Department of Radiology, Geisinger Medical Center, Danville, PA

<sup>7</sup>Department of Pathology and Laboratory Medicine, University of Pennsylvania, Philadelphia, PA

<sup>8</sup>Department of Cancer Biology, University of Pennsylvania, Philadelphia, PA

**Corresponding author:** Terence P. F. Gade  
Assistant Professor of Radiology and Cancer Biology  
University of Pennsylvania Perelman School of Medicine  
652 BRB II/III, 421 Curie Blvd  
Philadelphia, PA 19104-6160  
Tel: 215-573-9756  
Fax: 215-746-5511  
Email: [tgade@penncancer.upenn.edu](mailto:tgade@penncancer.upenn.edu)

**Manuscript type:** Original Manuscript

**Word count:** max 6000

**Number of figures/tables:** 4 figures, 1 table

**Keywords:** hepatocellular carcinoma,  $\beta$ -catenin, CTNNB1, transarterial chemoembolization (TACE), ischemia, embolization, bioenergetic homeostasis, oxidative metabolism

**Conflicts of interest:** KW, DT received research funding for Astra Zeneca through the Society of Interventional Oncology. SJH is a consultant for Boston Scientific, General Electric, and Siemen's Healthcare. GJN receives research funding from Sirtex Medical, Instylla, and Astra Zeneca. DEK receives research funding from Astra Zeneca, Roche Genetech, Exact Sciences, and Bausch. TPG is on scientific advisory board for Trisalus Life Sciences. The rest of the authors have declared no conflict of interest.

**Financial support:** This study was supported in part by the National Institutes of Health, National Cancer Institute, Grant R01CA234005 (TPG), the Society of Interventional Radiology Foundation's Pilot Grant (TPG), and Society of Interventional Radiology Foundation's Standardized/Structured Reporting Grant (KMW, GJN)

**Author's contributions:** KW, JAC, DT, and TPG participated in research design, performance of the research, data analysis, and writing of the article. DA, MK, SJH, GJN, and DEK participated in research design, performance of the research, data analysis, and editing of the paper. AW, WL, IG, DO, MCS, MD, SSN, JM, DS, SWS, SR, TK, EEF, and ESS participated in performance of the research and editing of the paper.

## ABSTRACT

**Background & Aims:** Transarterial chemoembolization (TACE) is the most common treatment for hepatocellular carcinoma (HCC) worldwide; however, response rates and durability vary widely. With the growing armamentarium of therapies for HCC patients, identifying predictors of response to TACE has become increasingly important for a patient population with limited hepatic reserve. We hypothesized that a distinct metabolic phenotype associated with  $\beta$ -catenin pathway mutations render HCC tumors more susceptible to TACE-induced ischemia.

**Material and Methods:** HCC patients referred for TACE were enrolled in a prospective cohort study at two academic medical centers from April 2016 to October 2021. Liver biopsies were acquired at the time of TACE, and mutational profiles were determined using next generation sequencing. Tumor response was determined by MRI using modified Response Evaluation Criteria in Solid Tumors. HCC cell lines with and without B-catenin mutations were grown in standard and ischemic cell culture conditions (1% O<sub>2</sub>, low nutrient media). Cell viability was measured by WST-1 reagent and Annexin-V PI assay. ATP concentration and metabolites were measured using CellTiter Glo and a YSI biochemical analyzer, respectively. Mitochondrial function was assessed through Seahorse XF Mito Stress Test.

**Results:** 53 HCC tumors from 50 HCC patients were biopsied prior to TACE, including 22/53 (41.5%) tumors with  $\beta$ -catenin pathway mutations. Despite larger tumor size (4.9 cm vs 3.0 cm  $p=0.01$ ), tumors with these mutations demonstrated increased rates of complete response after TACE at first imaging (9/22, 40.9% vs 6/31, 19.4%,  $p=0.06$ ) and best response (12/22, 54.5% vs 7/31, 22.6%,  $p=0.02$ ), as well as a longer time to tumor progression (median not yet reached vs 8.3 months,  $p=0.02$ ). *In vitro* modeling confirmed that  $\beta$ -catenin mutant HCC cells have reduced viability (21.4% vs 59.9%,  $p<0.01$ ) and ATP levels (8.47 vs 4.26 pM/cell,  $p<0.001$ ) under ischemic conditions compared to  $\beta$ -catenin wild type HCC cells.  $\beta$ -catenin mutant HCC cells had a dramatic increase in their susceptibility to glycolysis inhibition that was not seen in wild type HCC cells (0.09 vs 0.79 IC<sub>50</sub> ration for ischemic vs standard conditions,  $p=0.004$ ), suggesting a change from predominantly aerobic to anaerobic metabolism under ischemia specific to  $\beta$ -catenin mutant. This was further supported by increased sensitivity of  $\beta$ -catenin mutant cells to inhibition of the electron transport chain (43.9% vs 59.5%,  $p=0.02$ ,) as well as significantly higher basal oxygen consumption rates (0.74 vs 0.39 pmoles/min,  $p=0.04$ ), maximal respiratory capacity (1.46 vs 0.51 pmoles/min,  $p=0.01$ ) and ATP-linked respiration (0.58 vs 0.29 pmoles/min,  $p=0.04$ ).

**Conclusions:** HCC tumors with activating B-catenin pathway mutations demonstrate a superior response to TACE, driven by enhanced susceptibility to ischemia due to a greater dependence on oxidative phosphorylation for bioenergetic homeostasis. These findings hold the potential to provide a molecular basis for treatment selection in patients with HCC.

## **IMPACT AND IMPLICATIONS:**

With the growing armamentarium of locoregional and systemic therapies for patients with HCC, identifying predictors of response to individual therapies has become increasingly important for a patient population with limited hepatic reserve. Current treatment guidelines fail to incorporate molecular biomarkers to inform therapy. In a prospective clinical study of HCC patients undergoing transarterial chemoembolization (TACE), we demonstrated that tumors with activating mutations in the Wnt/B-catenin pathway have increased rates of complete response and longer time to local progression. We further characterized this finding *in vitro* by modeling the post-TACE ischemic environment and demonstrated that B-catenin mutant HCC cells have a distinct metabolic phenotype that renders this subtype more susceptible to ischemia. These findings provide the rationale for genotype-based strategies to enable precision medicine for patients with HCC patients.

## **GRAPHICAL ABSTRACT:**

## **HIGHLIGHTS:**

## **INTRODUCTION**

Hepatocellular carcinoma (HCC) is a leading cause of cancer-related mortality worldwide, as the majority of patients present with incurable disease and an associated survival of less than two

years.<sup>1-3</sup> This poor prognosis issues, in large part, from the significant heterogeneity of HCC tumors.<sup>4,5</sup> HCC develops through a multi-step process in a setting of chronic liver injury from diverse etiologies including viral hepatitis, alcohol or non-alcoholic steatohepatitis, and exposure to aflatoxin. The resulting molecular heterogeneity is underscored by the mutational landscape of HCCs which demonstrate an average of 30-40 mutations per tumor.<sup>6,7</sup> Aside from those in the TERT promoter, no mutation is observed in more than half of patients.<sup>7,8</sup> Advances in our understanding of the critical role these molecular signatures play in defining HCC biology have resulted in their incorporation into an emerging classification system for HCC. Specifically, a proliferative class enriched for poorly differentiated and highly proliferative tumors associated with *TP53* mutations and a non-proliferative class associated with moderately-to-well differentiated tumors and *CTNNB1* mutations.<sup>9,10</sup>

Despite these advances, there remains a narrow understanding of the influence of these molecular alterations on response to current treatments. Indeed, HCC stands out as one of the few malignancies for which molecular profiling informs neither staging nor management.<sup>11</sup> This deficiency stems in large measure from the limited role of biopsy in the care of patients with HCC, as a diagnosis can be made from clinical history and imaging alone. Recent retrospective studies demonstrating the predictive potential of molecular subtypes for standard-of-care therapies emphasize the importance of evolving these management paradigms to enable precision medicine strategies for patients with HCC.<sup>12-15</sup> Moreover, the development of novel systemic therapies, namely immune checkpoint inhibitors, and advances in endovascular locoregional therapies, including transarterial chemoembolization (TACE) and transarterial radioembolization (TARE), are revolutionizing HCC care. This growing armamentarium of HCC therapies further emphasizes the need for molecular biomarkers that can inform treatment selection, especially in a patient population with limited hepatic reserve.

Developed to maximize therapeutic effect in patients with HCC and underlying liver dysfunction, TACE is an endovascular locoregional therapy that delivers chemotherapy and embolic agents

by targeting branches of the hepatic artery that directly feed the tumor. Leveraging the liver's unique dual blood supply, TACE selectively promotes ischemia-induced tumor necrosis while sparing the surrounding liver parenchyma. TACE has been shown to improve survival in patients with unresectable HCC and is currently the most commonly used treatment for this population.<sup>16</sup> Despite its proven efficacy, response rates remain variable, and recurrence is common. Recent studies demonstrate the ability of HCC cells to survive TACE-induced ischemia through metabolic reprogramming, and suggest that this survival may differ between molecular subtypes.<sup>12,13,17,18</sup> To further explore these subtype specific differences, we performed a prospective clinical research study integrating pre-procedure biopsy for patients with unresectable HCC undergoing TACE. Observed differences in tumor responsiveness to TACE between molecular subtypes were then characterized *in vitro*, revealing distinct metabolic programs as an underlying mechanism.

## **METHODS**

### *Patient enrollment*

Adult patients with a clinical diagnosis of HCC referred for TACE were recruited from two tertiary care academic institutions from April 2016 to October 2021 and enrolled in an IRB-approved prospective cohort study prescribing HCC tumor biopsies immediately prior to TACE (University of Pennsylvania IRB #823696; Corporal Michael J Crescenz VA Medical Center IRB #01779; **Fig. 1**). TACE was performed at the time of biopsy to minimize the number of procedures for the patients and to mitigate the risk of bleeding. Patients were excluded if they (1) were a candidate for resection or liver transplantation; (2) had a tumor not amenable to biopsy by computed tomography (CT) or ultrasound (US)-guidance; (3) had prior treatment to the target HCC tumor; (4) did not have at least one post-treatment MRI.

### *Patient data collection and analysis*

Study data were prospectively collected and managed using Research Electronic Data Capture and Filemaker databases. Patient demographics, disease-specific information, and procedure details were obtained from chart review and discussion with the treating interventional radiologist. Histology slides were reviewed by hepatobiliary pathologist (EEF) with more than 25 years of experience for the presence of malignancy and grade of differentiation. All follow-up cross-sectional imaging was reviewed by a fellowship-trained body radiologist (ES) with more than 25 years of experience to determine the modified Response Evaluation Criteria in Solid Tumors (mRECIST) score for the targeted HCC tumor. Objective response rate was defined as complete (CR) or partial response (PR) by mRECIST divided by total. Best response date was defined as the date on which the target tumor either first had complete response or had the smallest diameter of enhancing tumor during the follow-up period. Time to target tumor progression was defined as months from date of best response to date of progression or last follow-up.

#### *Molecular profiling*

Genetic mutations were determined using a custom targeted sequencing amplicon panel developed in collaboration with Swift Biosciences. The assay targeted 234 genomic regions found to be commonly mutated in HCC using publicly available whole exome sequencing data. After generating libraries, samples were multiplexed at 20-30 samples per MiSeq sequencing run. SNVs and indels were called at allele frequencies >5% using the LoFreq variant caller.

#### *Bioinformatics*

TCGA expression matrices (tpm and STAR-Counts) and corresponding meta data for the "TCGA-LIHC" project were downloaded using the 'TCGAbiolinks' R package.<sup>1,2</sup>  $\beta$ -catenin gene (CTNNB1) mutation status data for TCGA-LIHC samples were downloaded using cBioPortal.<sup>3,4</sup> Samples were divided into groups based on mutation status of CTNNB1, filtering for "drivers". Differential gene expression analysis (DEG) was performed between the wild type and mutated

samples using the DESeq2 R package using the STAR-Counts expression data. Next, genes were ranked according to a composite score ( $-\log_{10}(\text{pvalue}) \times \text{sign}(\log_2\text{FoldChange})$ ) for gene set enrichment analysis (GSEA). GSEA was performed with the `clusterProfiler` R package using gene sets from MSigDB, Kegg and Gene Ontology (GO). Pathways were filtered for  $p < 0.05$  and manually curated based on pathway among all gene sets. Pathways with similar biological etiology among the three gene sets were plotted together. Heatmaps for genes of interest in relevant biological pathways were plotted using DESeq2 variance stabilizing transformed counts.

#### *Cell Lines and Culture Conditions*

$\beta$ -catenin mutant (SNU-398, HepG2) and wild type (Huh7, SNU-449) HCC cell lines were obtained from American Type Culture Collection (SNU-398, HepG2 and SNU-449, Manassas, VA) and the Japanese National Institutes of Biomedical Innovation, Health and Nutrition (Huh-7, Osaka, Japan). Given data suggesting the HepG2 cell line originated from a hepatoblastoma and lack of other established cell lines with B-catenin mutations, a primary cell line (21A2-PGM7567s3c1) generated in our lab from previously established patient-derived xenografts was also used to confirm findings.

Cells were cultured under standard (21% oxygen with RPMI media, 1% dialyzed FBS, 10 mM glucose, 2.05 mM glutamine) or ischemic conditions (1% oxygen with RPMI media, 1% dialyzed FBS, 1 mM glucose, 0.5 mM glutamine) as described previously. Cell viability was assessed using the cell proliferation reagent WST-1 (Roche, Basel, Switzerland) and flow cytometry using annexin V-FITC and propidium iodide (BD Biosciences, San Jose, CA). Cell counts were performed using a Countess II Cell Counter (Invitrogen, Waltham, MA). Glucose, lactate, glutamine, and glutamate concentrations were analyzed using a YSI biochemistry analyzer (Yellow Springs, OH), and ATP levels were quantified using the CellTiter-Glo Luminescent Cell Viability Assay (Promega, Madison, WI).

### *Pharmacologic inhibitors*

Etomoxir (Calbiochem, CAS 828934-41-4) was solubilized in DMSO and used for inhibition of fatty acid oxidation at 100  $\mu$ M, noting that concentrations  $\geq$  200  $\mu$ M have off-target effects.<sup>cit</sup>

Lactate dehydrogenase (LDH) inhibition was achieved using NCATS-SM1441, obtained from the National Cancer Institute (NCI, Bethesda, MD) and solubilized in Phosphate-Buffered Saline. Dose response curves were generated using 0.0001 to 100  $\mu$ M of NCATS-SM1441 and EC50 defined as concentration at which there was a 50% reduction in ATP generation. Rotenone was solubilized in DMSO and 50 nM concentration was used for inhibition of complex I of the electron transport chain *in vitro*.

### *Measurement of mitochondrial function*

Seahorse XF Cell Mito Stress Test Kit (#103015-100 Agilent, Santa Clara, CA) was used to compare mitochondrial function of HCC cells lines. Briefly, HCC cell lines were plated in dedicated 96-well plates at concentrations optimized to obtain 90-95% confluency 48 hours later when media was changed to assay media and cartridge was loaded with 2.5  $\mu$ M oligomycin, 1  $\mu$ M FCCP, and 0.5  $\mu$ M rotenone/antimycin. Plate was run on Seahorse Xfe96 and results were normalized to protein concentration per well.

### *Statistical Analysis*

For clinical data, medians of continuous variables were compared using the Kruskal Wallis test given lack of normal distribution, while categorical variables were compared using Pearson's Chi-squared test or Fisher's exact test as appropriate. Time to progression was calculated using Kaplan-Meier statistics. For *in vitro* experiments, comparisons between culture conditions and genetic subtypes were done using Student's t-tests. All data were analyzed using Stata/IC 16.1 and Prism 9.

## **RESULTS**



### *Wnt/B-Catenin pathway mutations are associated with superior outcomes following TACE*

50 patients with 53 HCC tumors underwent percutaneous core biopsy prior to TACE. The majority of patients were male (42/50, 84.0%) and white (32/50, 64.0%) with a median age of 64.4 years old (SD 8.1), consistent with the demographics of HCC patients in the United States (**Table 1**).<sup>cit</sup> Most patients had underlying cirrhosis (41/50, 82.0%) that was well compensated at the time of TACE (45/53, 84.9% Child-Pugh A) with median MELD of 8 (IQR 7-10). The majority of patients had BCLC stage B disease (28/53, 52.8%) with a median of 2 tumors (IQR 1-4) at time of enrollment and median targeted tumor size of 4.0 cm (IQR 2.5-6.3). Genomic profiling demonstrated activating Wnt/ $\beta$ -catenin pathway mutations in 22/53 tumors (41.5%).

Patients with Wnt/ $\beta$ -catenin pathway mutations had a higher proportion of underlying cirrhosis (18/22, 94.7% vs 23/31, 74.2%,  $p=0.13$ ), BCLC stage B disease (17/22, 77.3% vs 11/31, 35.4%,  $p = 0.006$ ), higher tumor number (3.5, IQR 1.75-6.25 vs 2, IQR 1-4,  $p<0.0001$ ), and a larger target tumor size (4.9 cm, IQR 3.5-8.1 cm vs 3.0 cm, IQR 2.1-4.6 cm,  $p=0.01$ ). Notably, tumors with Wnt/ $\beta$ -catenin pathway mutations were more often well-moderately differentiated HCC (19/22, 86.4% vs 16/29, 55.2%) with fewer cholangiocarcinoma (CCA) or combined HCC-CCA (1/22, 4.5% vs 4/29, 13.8%,  $p=0.14$ ). While there was no difference in overall response rate (ORR) at first imaging (20/22, 90.9% vs 26/31, 83.9%,  $p=0.69$ ) or at best response (21/22, 95.5% vs 28/31, 90.3%,  $p=0.63$ ), tumors with Wnt/ $\beta$ -catenin pathway mutations had higher rates of complete response (CR) at first imaging (9/22, 40.9% vs 6/31, 19.4%,  $p=0.12$ , **Fig. 2A**) and at best response (12/22, 54.5% vs 7/31, 22.6%,  $p=0.02$ , **Fig. 2B**). In addition, HCC tumors with Wnt/ $\beta$ -catenin pathway mutations were less likely to progress (4/18, 18.2% vs 15/31, 48.3%,  $p=0.02$ ) and demonstrated a longer time to progression (NYR vs 8.3 months,  $p=0.02$ , **Fig. 2C**). This remained true even if only tumors with pathology-confirmed HCC were included (NYR vs 6.6 months,  $p=0.02$ , **Supp Fig. ?**).

Given these findings and that nutrient deprivation is a driver of tumor cell death following TACE, we performed a gene set enrichment analysis to identify distinct metabolic signatures in this

HCC subtype. Analysis of publicly available RNA sequencing data from The Cancer Genome Atlas (TCGA) demonstrated that human HCC tumors with Wnt/ $\beta$ -catenin pathway mutations were enriched in the CTNNB1 subclass of HCC (Supplementary Fig. 1). These tumors exhibited increased expression of genes associated with the non-proliferative class of HCC, which correlates with genetic markers of improved survival (Supplementary Fig. 1), consistent with prior studies. Differential expression analysis of metabolic pathways revealed higher expression of gene sets involved in oxidative phosphorylation and mitochondrial metabolism, along with lower expression of genes involved in glycolysis and hypoxia signaling pathways compared to tumors without these mutations (**Fig. 2E, Supplementary Fig. 2**).

#### *Susceptibility of $\beta$ -Catenin Mutant HCC Cell Lines to Ischemia Correlates with Altered Bioenergetic Homeostasis*

To explore the influence of these differences in cellular responses to post-TACE microenvironment,  $\beta$ -catenin mutant (CTNNB1+: SNU-398, HepG2, 21A2) and  $\beta$ -catenin wild type HCC cell lines (CTNNB1-; SNU-449, Huh7) were grown in standard and ischemic culture conditions (**Fig. 3A**). Consistent with our clinical data, CTNNB1+ cell lines demonstrated markedly decreased cell viability under ischemic conditions compared to CTNNB1- cell lines (31.2% vs 84.6%,  $p < 0.0001$ , **Fig. 3B**). This finding was underscored by associated differences in bioenergetic homeostasis. Under standard conditions, HCC cells demonstrated similar levels of ATP per cell regardless of mutational background (8.47 vs 6.83 pM/cell,  $p = 0.34$ ); however, under ischemic conditions, ATP levels were significantly reduced in CTNNB1+ cell lines (8.47 vs 4.26 pM/cell,  $p < 0.001$ ) but not CTNNB1- cell lines (6.83 vs 6.43 pM/cell,  $p = 0.76$ , **Fig. 3C**). This reduction in ATP production was not associated with differential utilization of glucose in ischemic conditions (0.70 vs 0.68 nM/cell,  $p = 0.67$ , **Fig. 3D**). It was also not associated with differential utilization of glutamine under ischemic conditions, as measured by glutamine utilized

per cell (0.19 vs 0.21 nM/cell,  $p=0.81$ , **Fig. 3E**) or glutamate produced per utilized glutamine (0.52 vs 0.57 nM/nM,  $p=0.84$ , **Fig. 3F**).

#### *$\beta$ -catenin Mutant HCCs are More Susceptible to Inhibition of Glycolysis Under Ischemia*

To investigate differences in ATP synthesis between CTNNB1+ and CTNNB1- HCC cell lines, pharmacologic inhibitors targeting critical metabolic pathways were used on CTNNB1+ and CTNNB1- HCC lines under standard and ischemic conditions (**Fig. 4A**). There were no differences in ATP levels between CTNNB1+ and CTNNB1- HCC cells with inhibition of fatty acid oxidation under standard (89.7% vs 94.52% ATP reduction,  $p=0.31$ , **Fig. 4B**) or ischemic conditions (95.2% vs 88.4% ATP reduction,  $p=0.30$ , **Fig. 4C**). While there was no difference in ATP levels between CTNNB1+ and CTNNB1- HCC cells treated with LDH inhibitor, (32.5% vs 38.7% ATP reduction,  $p=0.63$ , **Fig. 4D**), CTNNB1+ cells had significantly decreased overall and per cell ATP levels with LDH inhibition under ischemic (71.6% vs 41.2%,  $p=0.0003$ , **Figure 4E**; 5.62 vs 2.38 nM/cell,  $p<0.0001$ , **Fig. 4F**). This resulted in a dramatic increase in susceptibility to LDH inhibition under ischemic conditions compared to standard conditions that was not seen in CTNNB1- HCC cells (0.09 vs 0.79 IC50 ration for ischemic vs standard conditions,  $p=0.004$ , **Fig. 4G**), suggesting a change from predominantly aerobic to anaerobic metabolism under ischemia specific to CTNNB1+ HCC cells.

#### *$\beta$ -catenin Mutant HCCs are Dependent on Oxidative Phosphorylation for Maintenance of ATP Levels*

To investigate this finding further, we inhibited oxidative phosphorylation with rotenone and demonstrated a significantly greater reduction in ATP levels in CTNNB1+ HCC cells compared to CTNNB1- HCC cells (43.9% vs 59.5%,  $p=0.02$ , **Fig. 5A**). To characterize evaluate for differences in the oxidative ATP synthesis, we measured oxygen consumption rates using the SeaHorse bioanalyzer and found that CTNNB1+ HCC cells incubated under standard conditions demonstrated higher levels of basal oxygen consumption rates (OCR) as compared to

CTNNB1<sup>-</sup> cells (0.74 vs. 0.39 pmol/min.,  $p=0.04$ , **Fig. 5B**) that correlated with greater levels of ATP-linked respiration (0.58 vs. 0.29 pmol/min.,  $p=0.04$ , **Fig. 5C**) as well as a nearly three-fold higher rate of maximal respiration (1.46 vs. 0.51 pmol/min.,  $p=0.01$ , **Fig. 5D**). These differences were further emphasized by a higher level of spare respiratory capacity (0.72 vs 0.12,  $p=0.03$ , **Fig. 5E**), and a greater than two-fold higher level of non-mitochondrial respiration (0.37 vs. 0.15 pmol/min.,  $p=0.003$ , **Fig. 5F**). In addition, CTNNB1<sup>+</sup> HCC cells demonstrated a greater level of respiration not coupled to ATP production (also known as proton leak) that did not reach statistical significance (0.16 vs. 0.10 pmol/min.,  $p=0.2111$ , **Fig. 5F**). Taken together, these findings point to an increased reliance in oxidative phosphorylation for ATP generation under standard conditions that results in greater susceptibility to glycolytic inhibition under ischemic conditions, a finding that could be leveraged to increase efficacy of TACE in this patient population.

## DISCUSSION

Leveraging a prospective clinical research protocol, we identified subtype-specific variations in response to TACE, the most commonly used treatment for HCC<sup>1</sup>. Our findings demonstrate that HCCs harboring activating  $\beta$ -catenin mutations exhibited significantly prolonged time to progression and higher rates of complete response compared to tumors lacking these mutations. Through analyses of data from The Cancer Genome Atlas, we observed distinct differences in the expression of metabolic genes in this molecular subtype. Specifically,  $\beta$ -catenin mutant HCCs exhibited elevated expression of oxidative phosphorylation-related genes, alongside reduced expression of glycolysis-related enzymes, suggesting that these tumors possess a unique metabolic profile that underpins their clinical behavior. In vitro experiments reinforced this hypothesis, revealing that  $\beta$ -catenin mutant HCC cells are particularly vulnerable to TACE-induced ischemia due to bioenergetic crisis precipitated by their reliance on oxidative

phosphorylation for ATP production. Collectively, these results establish  $\beta$ -catenin mutant HCCs as a unique metabotype that is particularly susceptible to ischemia following TACE.

While previously unreported in HCC, our findings align with studies describing subtype specific differences in cancer metabolism as well as metabolic differences between  $\beta$ -catenin and TP53 mutant cells. In contrast to TP53 mutations, which enhance glycolysis and suppress mitochondrial activity<sup>2</sup>,  $\beta$ -catenin signaling is closely linked to the activation of mitochondrial biogenesis, a process essential for sustaining the metabolic demands of rapidly proliferating cells. Studies have shown that Wnt/ $\beta$ -catenin signaling can stimulate mitochondrial biogenesis through various mechanisms, including the regulation of key mitochondrial genes and the modulation of mitochondrial dynamics and structure<sup>3</sup>. For instance, activation of  $\beta$ -catenin leads to an increase in mitochondrial number and enhanced mitochondrial function, facilitating oxidative phosphorylation and ATP production to meet the bioenergetic demands of tumor cells<sup>4</sup>. Consistent with this finding, our data suggest that  $\beta$ -catenin-mutant HCCs exhibit greater reliance on oxidative phosphorylation, with heightened mitochondrial activity and a reduced dependence on glycolysis to sustain their energy requirements. Further research is needed to elucidate the precise mechanisms by which  $\beta$ -catenin mutations promote or sustain oxidative phosphorylation in HCC.

These findings also highlight a critical deficiency in current treatment guidelines for HCC, which focus on disease burden and patient functional status without considering differences in disease biology. Although the therapeutic landscape for HCC has expanded significantly, outcomes remain poor, with the majority of patients experiencing disease progression following standard-of-care locoregional and systemic therapies<sup>5-9</sup>. This inconsistency is largely attributed to the heterogeneity of HCC, which arises from various genetic and environmental factors contributing to oncogenesis<sup>10, 11</sup>. On average, HCC tumors harbor 30-40 mutations, with only 15-25% containing targetable driver mutations, while  $\beta$ -catenin mutations are observed in approximately

30-40% of patients across studies<sup>12-15</sup>. Despite advances in our understanding of HCC's molecular biology, there remains a limited understanding of how this heterogeneity influences susceptibility to targeted therapies<sup>16, 17</sup>.

This limitation, along with the data presented here, highlights the potential of precision medicine strategies to address key challenges in the treatment of HCC. Recent studies underscore this potential by demonstrating subtype-specific differences in clinical responses to systemic and locoregional therapies. Consistent with our findings, a small study of primary and metastatic liver cancer showed that  $\beta$ -catenin pathway activation was associated with an increased response to TACE<sup>18</sup>. Additionally,  $\beta$ -catenin mutations have been linked to responses to immunotherapy. Tumors bearing these mutations may be enriched in the “immune-excluded” subtype of HCC, which is characterized by minimal tumor immune infiltration and low expression of checkpoint proteins, factors associated with decreased response to checkpoint inhibition<sup>17, 19</sup>. Collectively, these studies suggest that subtype-specific differences influence treatment response across various modalities, underscoring the need for improved diagnostics to aid in tumor phenotyping. Indeed, recently reported data demonstrating promising results for combination approaches incorporating TACE with immunotherapy highlight the need for biomarkers that can identify patients who will benefit most from these strategies.

The present study underscores the utility of biopsy in the management of HCC, offering critical insights into tumor grade, molecular characteristics, and driver mutations. In this study, tumor biopsy immediately prior to TACE demonstrated an acceptable risk profile, with a major complication rate of less than 2% (3/53, 1.8%; 2 bleeding events and 1 seeding event). The single instance of biopsy track seeding occurred in a patient whose pathology revealed cholangiocarcinoma (CCA), and notably, the seeding did not affect clinical outcomes. Furthermore, these biopsies provided other clinically significant findings—10% of lesions initially diagnosed as HCC were determined to be CCA or cHCC-CCA upon pathology review, a

discovery that could have influenced clinical management toward alternative therapies such as trans-arterial radioembolization, external radiation, or systemic chemotherapy. On imaging review by an expert radiologist, only one of these tumors was categorized as LIRADS M, with the others classified as LIRADS 5 or TIV. While fewer poorly differentiated HCC, CCA, or cHCC-CCA tumors were identified in the  $\beta$ -catenin mutation group, those harboring  $\beta$ -catenin pathway mutations still demonstrated higher rates of complete response at BR and longer time to progression compared to tumors without these mutations. These results remained consistent even when the analysis was restricted to biopsy-proven HCC tumors, suggesting that the inclusion of misdiagnosed CCA or cHCC-CCA tumors did not skew the overall findings (Supplemental Figure X).

Despite increasing evidence supporting the benefit of biopsy for characterizing tumor biology, invasive procedures in patients with compromised liver function and coagulopathies carry inherent risks, including a small but elevated risk of bleeding<sup>20</sup>. While biopsy prior to TACE allows for the potential embolization of bleeding vessels during the procedure, outpatient percutaneous biopsy does not typically provide this safeguard. This highlights the growing importance of less invasive approaches, such as liquid biopsies, which analyze circulating tumor DNA (ctDNA) or cell-free DNA<sup>21</sup>. These techniques offer a promising alternative, enabling real-time molecular profiling without the complications associated with tissue sampling. Additionally, molecular imaging techniques are emerging as non-invasive methods for assessing tumor biology and metabolic characteristics, providing actionable data at the time of initial diagnosis<sup>22</sup>.<sup>23</sup>. Notably, prior studies have demonstrated that  $\beta$ -catenin mutant HCCs exhibit increased choline uptake, corresponding to heightened accumulation of <sup>18</sup>F-fluorocholine<sup>24</sup> on PET imaging. The integration of liquid biopsy and molecular imaging into clinical practice could overcome the challenges of traditional biopsy, offering safer and more dynamic tools for personalizing treatment strategies in HCC.

Despite the observed link between  $\beta$ -catenin mutations and improved outcomes following TACE, our study did not demonstrate a significant survival advantage for patients with  $\beta$ -catenin mutant HCCs who underwent TACE. This lack of overall survival benefit may be attributed to several factors, including the relatively small sample size, variability in post-TACE treatments, and the inherent complexity of HCC biology. Co-occurring mutations, such as those involving TP53, may further complicate survival outcomes and confound our results. Future studies should aim to validate these findings in larger patient cohorts and explore the potential benefits of combining TACE with targeted therapies that exploit the metabolic vulnerabilities of  $\beta$ -catenin mutant tumors. Such approaches could involve the use of inhibitors of oxidative phosphorylation, which may amplify the effects of ischemia-inducing therapies like TACE.

This study includes several limitations in addition to a small sample size. Firstly, patients were recruited from two centers in close geographic proximity with a majority of HCCs arising in a background of HCV/alcohol-related cirrhosis. As a result, the reported population underrepresents the diverse etiologies of liver disease in which HCC arises. Secondly, the variability in TACE techniques across operators may limit the ability to extrapolate our findings.

In conclusion, this study establishes  $\beta$ -catenin mutant HCCs as a distinct metabolic subtype with heightened sensitivity to ischemia following TACE, driven by their reliance on oxidative phosphorylation for bioenergetic stability. While biopsy remains an important tool for identifying these molecular subtypes, the challenges associated with performing biopsy at the time of treatment highlight the potential of non-invasive alternatives, such as liquid biopsy and molecular imaging, for optimizing therapeutic strategies. Integrating molecular profiling earlier in the treatment process could not only personalize locoregional therapies like TACE but also guide the use of systemic and combination therapies tailored to specific tumor phenotypes. This approach promises to improve overall outcomes in HCC, addressing the tumor's heterogeneity and allowing for more precise, targeted interventions across a broader spectrum of therapeutic



modalities. Given the diversity of locoregional therapies, our findings underscore an opportunity for interventional oncologists to play a leading role in the development of precision medicine for HCC.

## References

1. Bray, F. *et al.* Global cancer statistics 2018: GLOBOCAN estimates of incidence and mortality worldwide for 36 cancers in 185 countries. *CA. Cancer J. Clin.* **68**, 394–424 (2018).
2. Scudellari, M. Drug Development: Try and try again. *Nature* **516**, S4–S6 (2014).
3. Llovet, J. M., Villanueva, A., Lachenmayer, A. & Finn, R. S. Advances in targeted therapies for hepatocellular carcinoma in the genomic era. *Nat. Rev. Clin. Oncol.* **12**, 408–425 (2015).
4. Jovel, J. *et al.* A Survey of Molecular Heterogeneity in Hepatocellular Carcinoma. (2018) doi:10.1002/hep4.1197/full.
5. Llovet, J. M. & Hernandez-Gea, V. Hepatocellular carcinoma: Reasons for phase III failure and novel perspectives on trial design. *Clin. Cancer Res.* **20**, 2072–2079 (2014).
6. Villanueva, A. & Llovet, J. M. Liver cancer in 2013: Mutational landscape of HCC - The end of the beginning. *Nature Reviews Clinical Oncology* vol. 11 73–74 (2014).
7. Guichard, C. *et al.* Integrated analysis of somatic mutations and focal copy-number changes identifies key genes and pathways in hepatocellular carcinoma. *Nat. Genet.* **44**, 694–698 (2012).
8. Schulze, K. *et al.* Exome sequencing of hepatocellular carcinomas identifies new mutational signatures and potential therapeutic targets. *Nat. Genet.* **47**, 505–511 (2015).
9. Calderaro, J. *et al.* Histological subtypes of hepatocellular carcinoma are related to gene mutations and molecular tumour classification. *J. Hepatol.* **67**, 727–738 (2017).
10. Raja, A. & Haq, F. Molecular classification of hepatocellular carcinoma: prognostic importance and clinical applications. *J. Cancer Res. Clin. Oncol.* **148**, 15–29 (2022).
11. Reig, M. *et al.* BCLC strategy for prognosis prediction and treatment recommendation: The 2022 update. *Journal of Hepatology* vol. 76 681–693 (2022).
12. Ziv, E. *et al.* Gene Signature Associated with Upregulation of the Wnt/ $\beta$ -Catenin Signaling Pathway Predicts Tumor Response to Transarterial Embolization. *J. Vasc. Interv. Radiol.* **28**, 349-355.e1 (2017).
13. Ziv, E. *et al.* NRF2 dysregulation in hepatocellular carcinoma and ischemia: A cohort study and laboratory investigation. *Radiology* **297**, 225–234 (2020).
14. Zhu, A. X. *et al.* Molecular correlates of clinical response and resistance to atezolizumab in combination with bevacizumab in advanced hepatocellular carcinoma. *Nat. Med.* **28**, 1599–1611 (2022).

15. 15. Harding, J. J. *et al.* Prospective genotyping of hepatocellular carcinoma: Clinical implications of next-generation sequencing for matching patients to targeted and immune therapies. *Clin. Cancer Res.* **25**, 2116–2126 (2019).
16. 16. Llovet, J. M. & Bruix, J. Systematic review of randomized trials for unresectable hepatocellular carcinoma: Chemoembolization improves survival. *Hepatology* **37**, 429–42 (2003).
17. 17. Gade, T. P. F. *et al.* Ischemia induces Quiescence and autophagy Dependence in hepatocellular carcinoma. *Radiology* **283**, (2017).
18. 18. Perkons, N. R. *et al.* Hyperpolarized Metabolic Imaging Detects Latent Hepatocellular Carcinoma Domains Surviving Locoregional Therapy. *Hepatology* **72**, 140–154 (2020).
- 19.

**\*Abbreviations:**

AFP: alpha-fetoprotein; BCLC stage: Barcelona clinic liver cancer stage; CT: computed topography; CCA: cholangiocarcinoma; HCC: hepatocellular carcinoma; cHCC-CCA: combined hepatocellular and cholangiocarcinoma; FDG PET: fluorodeoxyglucose positron emission tomography; HCV: hepatitis C virus; HBV: hepatitis B virus; IRB: institutional review board; IQR: interquartile range; LIRADS score: liver reporting and data system score; LRT: locoregional therapy; MELD: model for end-stage liver disease; MRI: magnetic resonance imaging; NAFLD: non-alcoholic fatty liver disease; PDX: patient-derived xenografts; SD: standard deviation; TERT: telomerase reverse transcriptase; ultrasound: US;

**Acknowledgements:**

Research reported in this publication was supported in part by NIH (R01CA234005) and Society of Interventional Oncology-Guerbet Pilot Grant funding.

<b>Table 1. Patient Characteristics</b>				
	<b>Total (n=53)</b>	<b>Wnt pathway mutation (n=22)</b>	<b>No Wnt pathway mutation (n=31)</b>	<b>p-value</b>
<b>Age (SD)</b>	64.4 (8.1)	65.1 (6.9)	63.9 (8.9)	0.64
<b>Gender (%)</b>				0.47
Male	39 (83.0)	15 (88.2)	24 (80.0)	
Female	8 (17.0)	2 (11.8)	6 (20.0)	
<b>Race/ethnicity (%)</b>				0.44
White	31 (66.0)	13 (76.5)	18 (60.0)	
Black/African American	11 (23.4)	3 (17.6)	8 (26.7)	
Asian	3 (6.4)	0	3 (10.0)	
Other	2 (4.3)	1 (5.9)	1 (3.3)	
<b>Etiology of HCC (%)</b>				0.13
HCV	25 (53.2)	11 (70.6)	13 (43.3)	
Alcohol	6 (12.8)	3 (17.6)	3 (10.0)	
NAFLD	6 (12.8)	0	6 (20.0)	
HBV	3 (6.4)	1 (5.9)	2 (6.7)	
Other	2 (4.3)	1 (5.9)	1 (3.3)	
Unknown	5 (10.6)	0	5 (16.7)	
<b>Underlying cirrhosis (%)</b>	39 (83.0)	17 (100)	22 (73.3)	0.04*
<b>MELD score (IQR)</b>	8 (7-10)	9 (8-10)	8 (7-10)	0.41
<b>Childs-Pugh score (%)</b>				0.93
A	39 (83.0)	14 (82.4)	25 (83.3)	
B	8 (17.0)	3 (17.6)	5 (16.7)	
<b>BCLC Stage (%)</b>				0.03*
A	11 (23.4)	1 (5.9)	10 (33.3)	
B	24 (51.0)	13 (76.5)	11 (36.7)	
C	12 (25.5)	3 (17.6)	9 (30.0)	
<b>AFP (ng/mL, IQR)</b>	14 (5-270)	14 (6-175)	13 (5-381)	0.93
<b># of lesions</b>	2 (1-4)	3.5 (1.75-6.25)	2 (1-4)	<0.0001*
<b>Size of lesion (cm, IQR)</b>	4.0 (2.5-6.3)	4.9 (3.5-8.1)	3.0 (2.1-4.6)	0.01*
<b>Location of lesion</b>				0.04*
Right lobe (%)	39 (73.6)	19 (86.4)	20 (64.5)	
<b>Pathology</b>				0.14
Well/mod differentiated HCC	35 (68.6)	19 (86.4)	16 (55.2)	
Poorly differentiated HCC	4 (7.8)	1 (4.5)	3 (10.3)	
CCA or cHCC/CCA	5 (9.8)	1 (4.5)	4 (13.8)	
No malignancy	7 (13.7)	1 (4.5)	6 (20.7)	

**Figure 1: Patient enrollment schematic.**

### **Figure 2: Improved outcomes post-TACE in Wnt/B-catenin mutant HCC**

Target tumor response to TACE measured by mRECIST at first imaging (**A**) and best response (**B**) between tumors with Wnt/B-catenin pathway mutations (red) compared to tumors without these mutations (white). Probability of target tumor progression from time of best response (**C**). Pathway enrichment analyses of the top differentially expressed genes in Wnt/ $\beta$ -catenin pathway mutant HCCs versus tumors without these mutations (**D**).

### **Figure 3: B-catenin mutant HCC cells are more susceptible to ischemia**

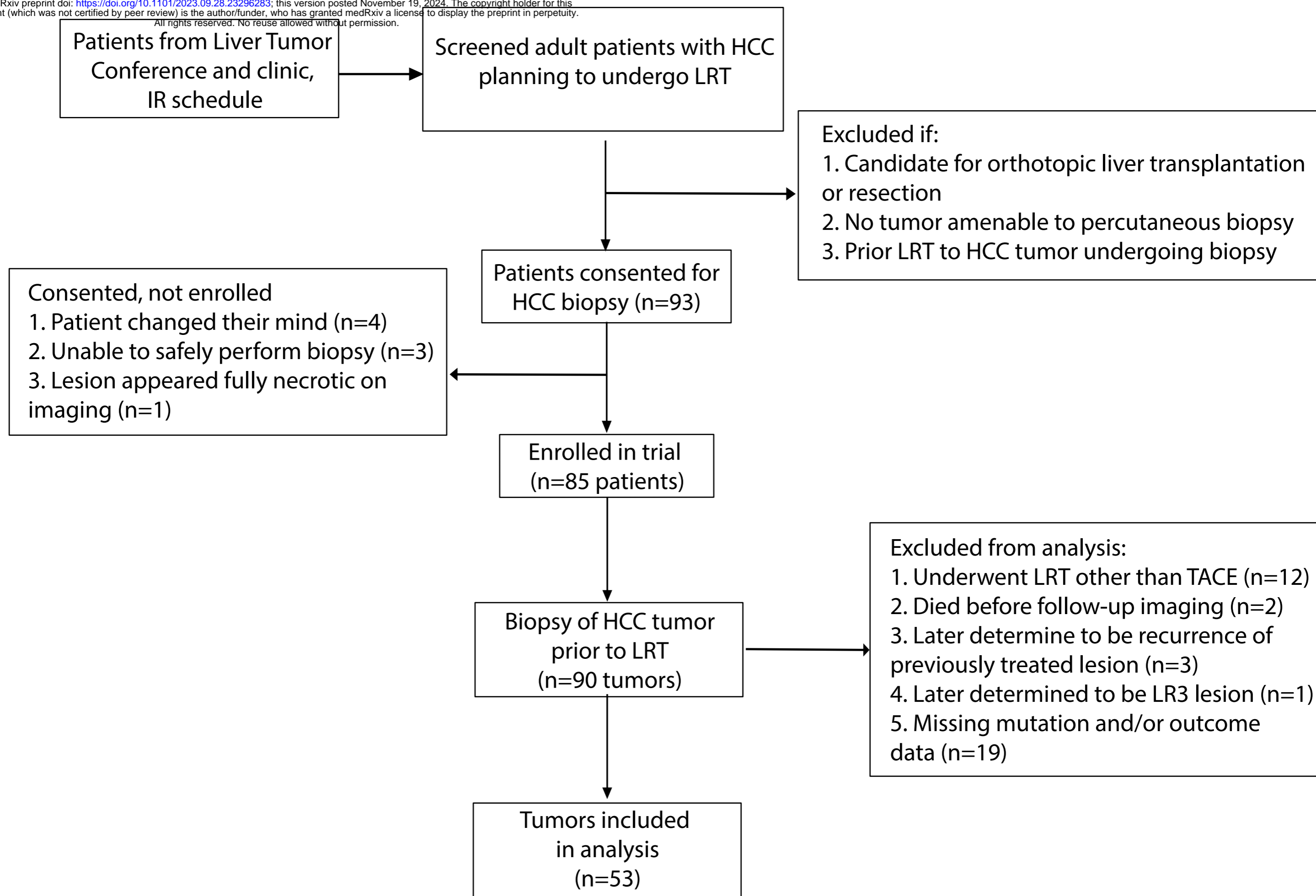
Schematic of *in vitro* conditions (**A**). Percentage of viable cells measured by flow cytometry after 72 hours in standard (S) and ischemic (I) conditions for B-catenin wildtype (WT) and mutant (MUT) cell lines (**B**). ATP levels per cell measured by CellTiterGlo at 12 hours (**C**). Glucose utilized per cell at 12 hours using YSI analyzer (**D**). Glutamine utilized per cell at 12 hours using YSI analyzer (**E**). Glutamate produced per utilized glutamine at 12 hours using YSI analyzer (**F**).

### **Figure 4: B-catenin mutant HCC cells become more glycolysis-dependent under ischemia**

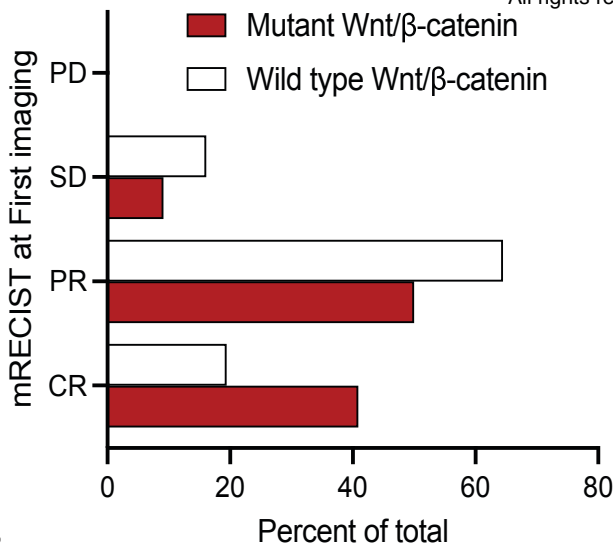
Schematic of mechanisms of ATP production (A). Change in ATP levels measured by CellTiterGlo after treatment with etomoxir under standard (B) and ischemic conditions (C) for B-catenin wildtype (WT) and mutant (Mut) HCC cell lines. Change in ATP levels measured by CellTiterGlo after treatment with LDH inhibitor under standard (D) and ischemic conditions (E). ATP levels per cell measured by CellTiterGlo at 12 hours under ischemia (G). Ratio of IC50 under ischemia to IC50 under standard conditions for LDH inhibitor.

**Figure 5: B-catenin mutant HCC cells depend on oxidative generation of ATP**

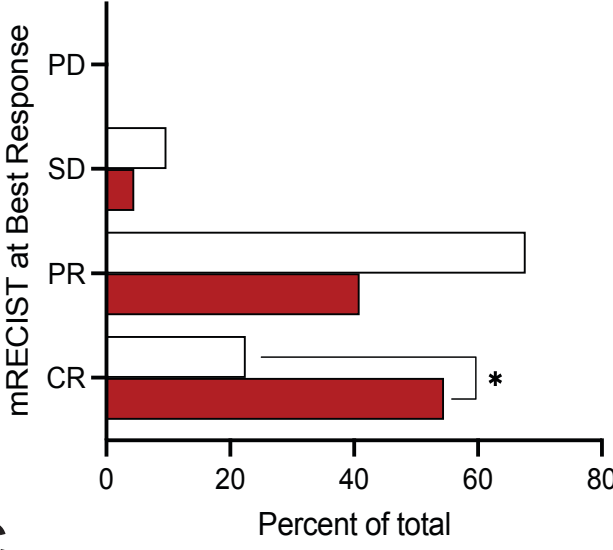
Change in ATP levels measured by CellTiterGlo after treatment with rotenone, a complex I inhibitor, under standard conditions (**A**) for B-catenin wildtype (WT) and mutant (Mut) HCC cell lines. Oxygen consumption rates measured by Seahorse Mito Stress Kit for basal respiration (**B**), ATP-linked respiration (**C**), maximal respiration (D), spare capacity (**E**), and non-mitochondrial respiration (**F**).



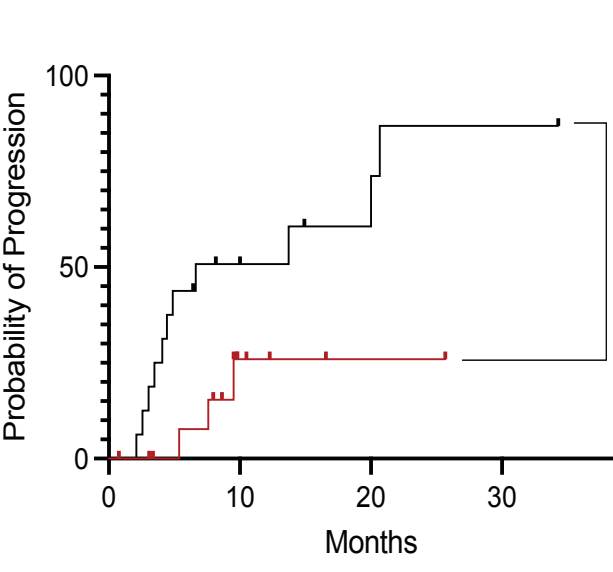
A



B

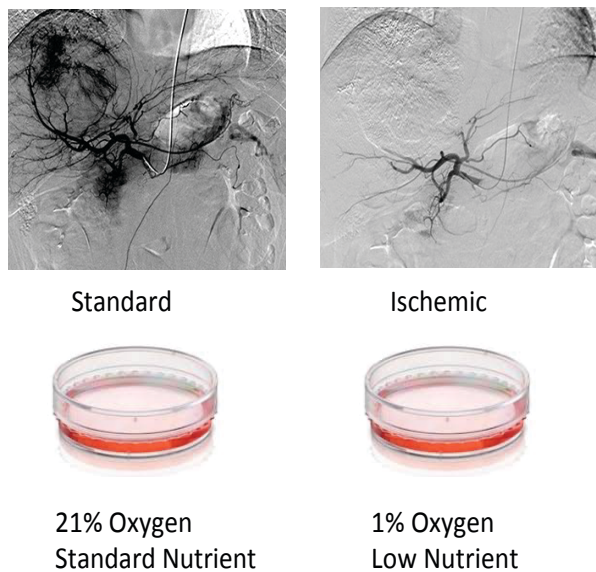
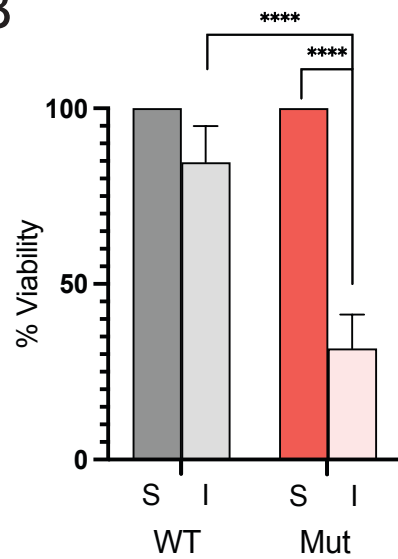
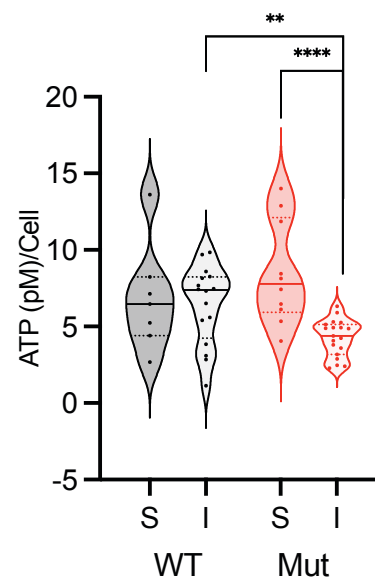
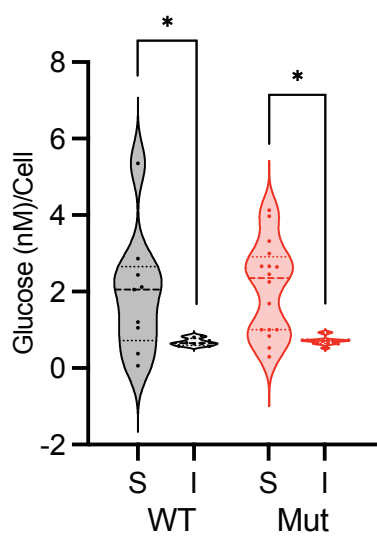
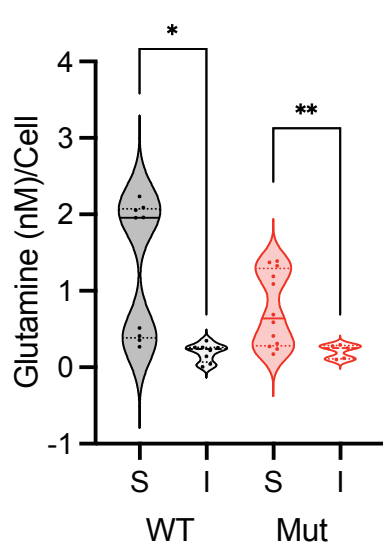
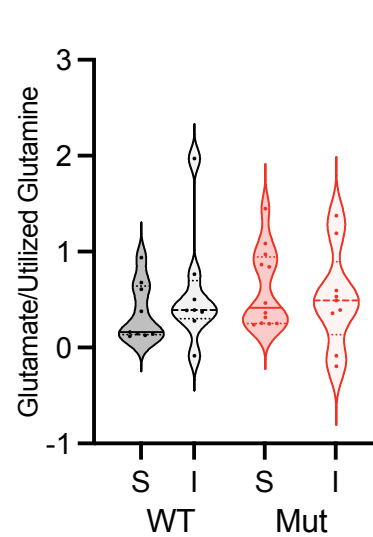


C

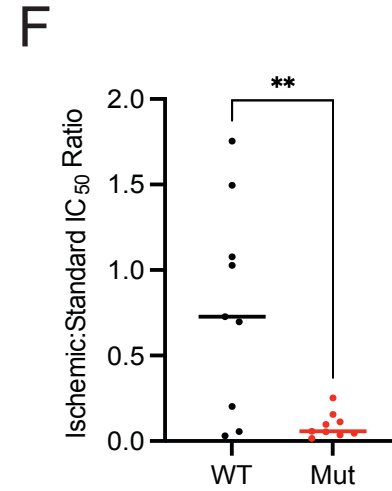
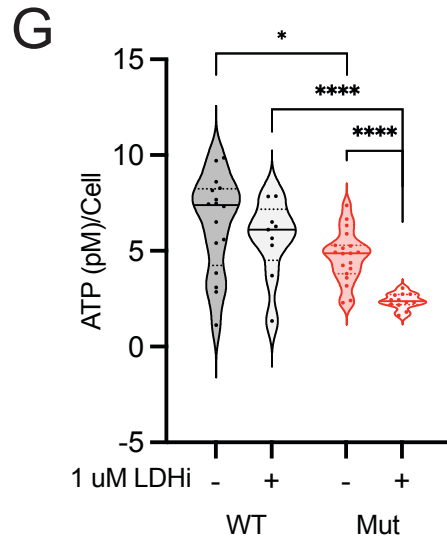
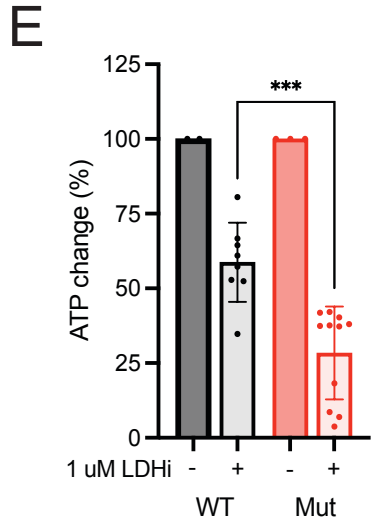
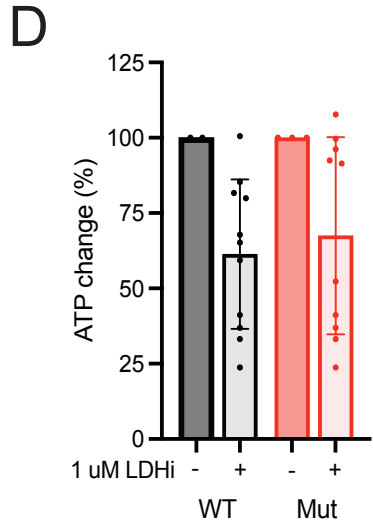
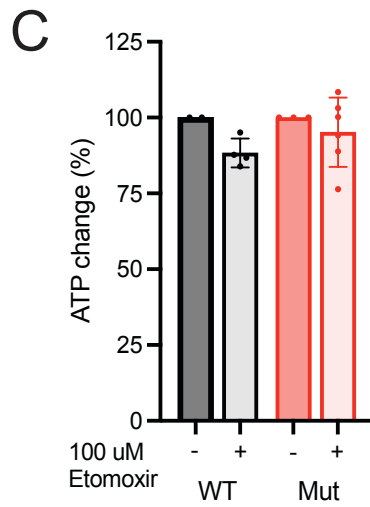
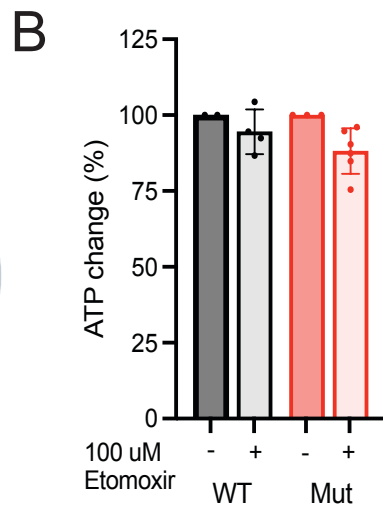
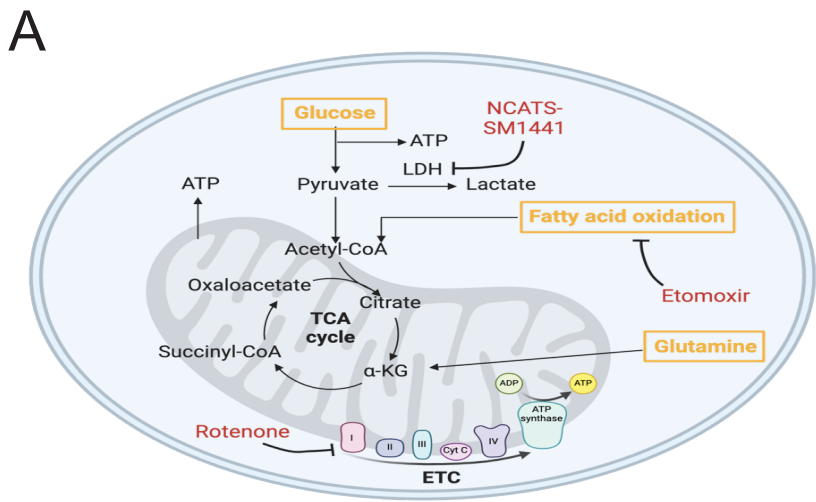


D

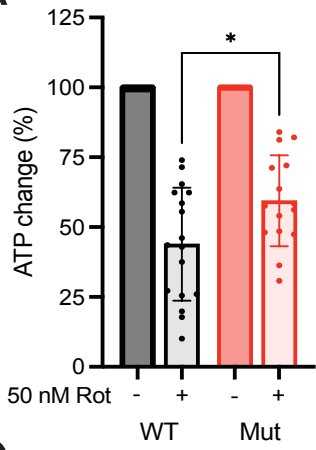


**A****B****C****D****E****F**

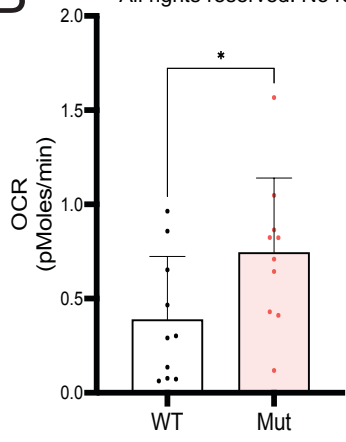




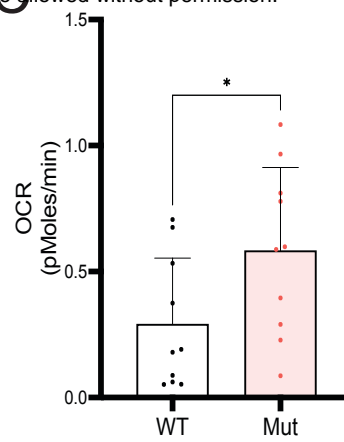
A



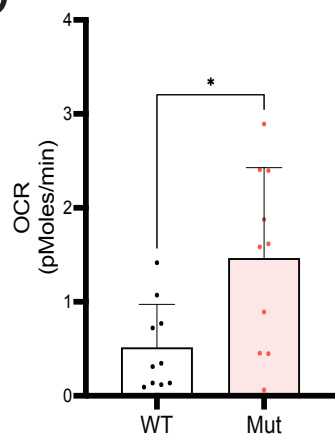
B



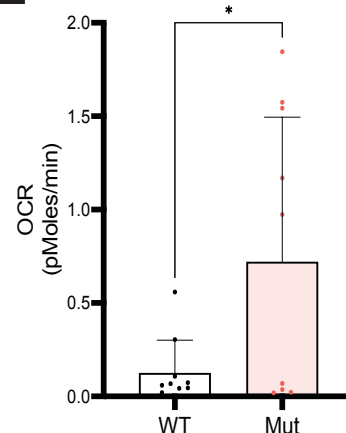
C



D



E



F

